European Review for Medical and Pharmacological Sciences 2022; 26: 4001-4015

Markedly decreased growth rate and biofilm formation ability of *Acinetobacter schindleri* after a long-duration (64 days) spaceflight

P. BAI[1], Y. LI[2], J. BAI[1], H. XU[3]

[1]Department of Respiratory Diseases, PLA Rocket Force Characteristic Medical Center, Beijing, China
[2]Department of Gastroenterology, First Medical Center, [3]Department of Cardiology, Second Medical Center, Chinese PLA General Hospital, Beijing

Po Bai, Yi Li and Jie Bai contributed equally to this work

Abstract. – OBJECTIVE: The objective of this study was to investigate the effects of long-duration space flight on the biological characteristics of *Acinetobacter schindleri* (*A. schindleri*).

MATERIALS AND METHODS: In this study, an *A. schindleri* strain was collected from condensate water of the Shenzhou-10 spacecraft and then was sent into space again to the Tiangong-2 space lab for a long-duration spaceflight (64 days). Later, the impacts of the long-duration spaceflight on phenotype, genome and transcriptome of *A. schindleri* were analyzed.

RESULTS: It was found that the long-duration spaceflight markedly decreased the growth rate and biofilm formation ability of *A. schindleri*. Furthermore, comparative genomic and transcriptomic analyses revealed that the decreased growth rate might be associated with differentially expressed genes (DEGs) involved in transmembrane transport, energy production and conversion, and biofilm was reduced due to downregulation of the pil and algR genes.

CONCLUSIONS: The findings are of major importance for predicting bacterial pathogenesis mechanisms and possible spacecraft contamination during long-duration spaceflights in the future.

Key Words:
Acinetobacter schindleri, Long-duration spaceflight, Biofilm formation, Growth rate, genome, Transcriptome.

Introduction

With the exploration of the universe and the development of the field of space life science, the space environment has become a new area for human activities. During human space exploration, microorganisms are unavoidably introduced into the spacecraft by astronauts and proliferate in the air and assembly facilities of the space station[1-3]. However, due to the severe conditions of the space environment, such as microgravity, cosmic radiation, and low nutrient levels, microorganisms undergo many physiological and biological alterations related to processes such as growth rate, virulence, biofilm formation, antibiotic susceptibility and metabolism[4-7]. Various changes of microorganisms in the space environment not only affect host-microbe interactions but also influence the corrosion of space vehicles and space stations[8,9]. Since the first launch of the Salyut 1 space station by the Soviet union in 1971, microbial contamination in space stations has become one of the most important monitored issues, and much attention has been paid to solve this problem in space environments[10,11]. Thus, studying the changes of microbes in a space environment is important for both astronaut health and spacecraft protection.

Acinetobacter schindleri (*A. schindleri*) is a Gram-negative bacterium that exists in a wide range of natural environments, such as soil, water and air[12]. It is an opportunistic pathogen that can cause infectious diseases, such as bacteremia, mainly in immune-deficient people[13], and can also induce infection in the space environment, given that the immune system of astronauts is significantly impaired during spaceflight[13,14]. In addition, *A. schindleri* has a strong adhesive ability, which makes it easy to adhere to the surface of inanimate materials[15]. It can produce biofilms and cause corrosion to metallic materials, ultimately influencing the safe operation of the spacecraft.

Corresponding Author: Po Bai, MD; e-mail: baipo0220@outlook.com

China's space station will be launched in the early 2020s, which might provide a platform for long-duration studies to examine the impact of microbes in the space environment on human health and spacecraft safety. This mission requires that Chinese astronauts stay on the space station for at least 6 months with little or no opportunity for emergency medical evacuation of sick crew members. It has been reported that crew members after a long-duration mission experience significant functional immune dysregulation compared with those after a short-duration mission[16]. Moreover, microorganisms possess the ability to impact human life during or after long space missions, both positively and negatively[17,18]. Therefore, it is of crucial importance to understand the impact of long-duration spaceflight on the behavior of microorganisms that will inevitably have access to the space environment along with the human body and equipment. In 2002, China began to perform a space microbiology experiment, and *Monascus purpureus* was the first microbe carried into the space environment by the Shenzhou-3 spacecraft[19]. Although information regarding the effect of the space environment on microorganisms has gradually accumulated, little data exist on the changes in microbial behavior after a long-duration spaceflight because of the limitations of spaceflight time.

The purpose of this study was to observe the effect of a long-duration spaceflight on the biological characteristics of *A. schindleri*. An *A. schindleri* strain was collected from the condensate water of the Shenzhou-10 manned spacecraft after a short-duration spaceflight (15 days) and then sent to the space environment again using the Tiangong-2 space lab for a long-duration spaceflight (64 days). The phenotypic, genomic and transcriptomic characteristics of *A. schindleri* were analyzed to detect the variations in microbial behavior and underlying mechanisms after a long-duration spaceflight.

Materials and Methods

Bacterial Strains and Culture Conditions

The original *A. schindleri* strain (designated H3) was obtained from the condensate water of the Shenzhou-10 manned spacecraft that was in space environment from June 11, 2013 to June 26, 2013. After returning to Earth, the *A. schindleri* strain was stored at -80°C immediately and then inoculated into plastic containers filled with Luria-Bertani (LB) medium before the launch of the Tiangong-2 space lab. The special plastic containers were designed for this experiment as previously reported[20]. The LB medium contained yeast extract (5 g/l), tryptone (10 g/l), NaCl (10 g/l), and agar powder (15 g/l), and the pH of the medium was adjusted to 7.0-7.2[21]. The cultured *A. schindleri* strain (designated ST12) was transported to the Jiuquan Satellite Launch Center by a military helicopter and launched into space by the Tiangong-2 space lab at 22:04 on September 15, 2016, and finally grew at the cabin temperature after reaching into orbit. The Tiangong-2 space lab was successfully docked with the Shenzhou-11 manned spacecraft at 03:31 on October 19. The Shenzhou-11 manned spacecraft and Tiangong-2 space lab remained connected for 30 days at an approximate apogee distance of 393 km. Then, the growth of the samples was terminated when the return capsule of the Shenzhou-11 manned spacecraft completed the experimental task and left the Tiangong-2 space lab at 12:41 on November 17. The return capsule landed at Siziwang Banne at 14:07 on November 18, 2016. The microbiological samples were quickly transported to Beijing by a military plane and reached the laboratory of the Chinese PLA General Hospital at 20:02 on November 18. In parallel, the cultured *A. schindleri* strain (designated GT12) were placed on the ground as the control experiment, and the temperature data obtained by measuring devices equipped in the cabin of spacecraft were recorded each hour and ranged from 19°C to 23°C. After the manned spacecraft landed on Earth, both ST12 and GT12 were immediately grown on solid agar plates for further research.

Phenotypic Analysis

Preparation

The subcultures were measured by a turbidimeter (Biomérieux, Marcy-l' Étoile, France), which was adjusted to 0.5 McF (~10^8 CFU/mL). Then, they were diluted into different concentrations as needed for growth rate, biofilm formation and antibiotic susceptibility tests.

Growth Rate Assay

Growth curves of ST12 and GT12 were plotted at 600 nm in a Bioscreen C system (Lab Systems, Finland). The strains were cultivated in LB liquid medium at 37°C overnight. 20 μL of suspension

sample with a concentration of ~10^6 CFU/ml was inoculated into a 96-well microtiter plate, incubated with 350 µL of LB liquid medium per well and continuously shaken at the maximum intensity for 32 h. The optical density (OD) value at 600 nm was measured every 2 h using a Thermo Multiskan Ascent (Thermo Fisher Scientific, Waltham, MA, USA). A well with only 370 µL of LB liquid medium was also included as a blank control.

Antibiotic Susceptibility Test

Both ST12 and GT12 were tested for susceptibility to 10 antimicrobial susceptibility test discs (Oxoid Limited, Basingstoke, UK), namely, trimethoprim sulfamethoxazole (SXT, 25 µg), ciprofloxacin (CIP, 5 µg), levofloxacin (LEV, 5 µg), piperacillin and tazobactam (TZP, 110 µg), cefoperazone and sulbactam (SCF, 105 µg), imipenem (IPM, 10 µg) and aztreonam (ATM, 30 µg), cefepime (FEP, 30 µg), amikacin (AK, 30 µg), and meropenem (MEM, 10 µg) using the disk diffusion method. The surface of the LB agar plate was covered with bacterial inoculum (~10^8 CFU/mL), and the antibiotic disks were put on the surface of the plate. Next, the inhibition zone diameter was measured to determine the antibiotic sensitivity of the bacteria according to standard specifications after incubation for 24 h at 37°C. *E. coli* strain ATCC 25922 and *P. aeruginosa* strain ATCC 27853 were used as quality strains.

Biofilm Formation Assay

Two hundred microliters of the bacterial inoculum (~10^7 CFU/ml) were inoculated into a 96-well polystyrene microtiter plate and cultivated at room temperature (~25°C) for 48 h. Then, the microtiter plate was washed three times using phosphate-buffered saline (PBS, pH = 7.4). After fixation with methanol and air drying, the remaining bacteria were stained with 200 µL of 0.1% crystal violet (Sigma-Aldrich, St. Louis, MO, USA) for 20 min. Subsequently, the microtiter plate was washed with PBS to remove excessive crystal violet. After air drying, the stained samples were dissolved in 95% ethanol and were measured by OD value at 570 nm using a Thermo Multiskan Ascent (Thermo Fisher Scientific, Waltham, MA, USA).

Genome Sequencing and Assembly

The genomic DNAs of H3, GT12 and ST12 were isolated by the sodium dodecyl sulfate (SDS) extraction method. After quality control by electrophoretic detection, the extracted DNAs were quantified by a Qubit 2.0 fluorometer. Genomic sequencing and library construction were performed by Beijing Novogene Bioinformatics Technology Company. A 10 kb SMRT Bell library was constructed, and whole-genome sequencing was performed on the PacBio RSII platform. High-quality reads were acquired using the genome assembler SMRT 2.3.0, and short reads were assembled to generate one contig without gaps[22,23]. Finally, data were uploaded to GenBank, and accession numbers of the complete genome of H3 strain were CP030754-CP030758.

Genome Component Prediction

Gene components, including coding genes, interspersed and tandem repetitive sequences, noncoding RNA, genomic islands, prophages and clustered regularly interspaced short palindromic repeat (CRISPR) sequences, were predicted. The specific steps were carried out as follows: (1) related coding genes were predicted by the GeneMarkS program; (2) interspersed repetitive sequences were analyzed by the RepeatMasker and tandem repetitive sequences were retrieved by the Tandem Repeats Finder; (3) transfer RNA (tRNA) genes, ribosomal RNA (rRNA) genes, and small nuclear RNA (snRNA) genes were predicted by tRNAscan-SE, rRNAmmers and BLAST against the Rfam database, respectively; (4) genomic islands were analyzed by the IslandPath-DIOMB program; (5) prophages were predicted by the phiSpy program; and (6) CRISPR identification was performed by the CRISPRFinder.

Genome Function Analysis

Five databases, namely, the Gene Ontology (GO), Kyoto Encyclopedia of Genes and Genomes (KEGG), Clusters of Orthologous Groups (COG), Non-Redundant Protein (NR) and Swiss-Port databases were used to predict gene functions. A whole-genome BLAST search was performed against five databases.

Whole-Genome Map Drawing

The whole-genome map of H3 was created by the CIRCOS software[24], and the genome sequencing statistics are shown on the map.

Comparative Genomic Analysis

The genomes of ST12 and GT12 were sequenced using high-throughput sequencing Illumina technology. A paired-end library with an

insert size of 350 bp was constructed for each DNA sample. The paired-end library was sequenced using an Illumina HiSeq 4000 by the PE150 strategy. Quality control of the paired-end reads was performed using an in-house program. Raw data were filtered, and low-quality data were removed. Finally, clean data were used for read mapping. BWA software was used to map the read to the reference sequence, and SAMTOOLS software was utilized to count the coverage of the reference sequence for the read and explain the alignment results. Besides, SNPs (single nucleotide polymorphisms) and InDels (insertions and deletions) were detected by the genomic alignment results using the SAMTOOLS software mentioned above. The whole-genome mutation profile was created by CIRCOS software, and the read coverage and distribution of the SNPs and InDels are shown in the genome mutation profile. Ultimately, data were uploaded to GenBank, and accession numbers for resequencing data of GT12 and ST12 were SRR7415022 and SRR7415023, respectively m while those for transcriptomic data of GT12 and ST12 were 398 SRR7410979 and SRR7410978, respectively.

Sequencing and Filtering

Total RNA samples were isolated immediately from the cells incubated in semisolid LB medium using a RNeasy Protect Bacteria Mini Kit (QIAGEN, Hilden, Germany) following the standardized protocols. After measuring the integrity and purity of the RNA samples, a cDNA library was generated using NEBNext Ultra Directional RNA Library Prep Kit for Illumina (NEB, Ipswich, MA, USA) according to the manufacturer's instructions. The library was diluted to 0.1 ng/µl after initial quantification by a Qubit 2.0 fluorometer. Then, the insert size of the library was verified by the Agilent 2100 system, and the effective concentration of the library was quantified accurately using the Q-PCR method. Library sequencing was performed using the Illumina HiSeq™ 2500 platform. Clean reads were obtained by removing adapter reads, poly-N reads and low-quality reads from the raw data. Data have been uploaded to GenBank. Accession numbers for transcriptomic data of GT12 and ST12 are SRR7410979 and SRR7410978, respectively.

Gene Expression Value Analysis

The reference genome was built, and the paired-end reads were mapped to a reference sequence using Bowtie 2[25]. The gene expression level of each sample was analyzed by HTSeq software. FPKM was used to calculate the gene expression level according to gene length and sequencing depth. Moreover, DESeq software was used to analyze differential gene expression, and genes yielding p-values < 0.05 upon DESeq analysis were defined as differentially expressed genes (DEGs).

Functional Annotation and Enrichment Analysis

GO functional annotation and COG functional annotation of DEGs were performed using GOseq software and Blastall software, respectively. Terms with p-values < 0.05 were considered significantly enriched by DEGs.

Statistical Analysis

Each phenotypic experiment was performed in triplicate and repeated at least three times. The data were represented as mean ± standard deviation (SD). Statistical comparison of the data was conducted using one-tailed Student's t-test. GraphPad Prism (version 7.00, La Jolla, CA, USA) was used for data analysis. Differences with p-values < 0.05 were considered statistically significant.

Results

Phenotypic Characteristics

Growth Rate

OD values of ST12 and GT12 at 600 nm are measured every 2 h for a period of 32 h. Growth curves of ST12 and GT12 are shown in Figure 1. Compared with GT12, ST12 exhibited a decreased growth rate, especially after 10 h ($p = 0.0037$).

Antibiotic Susceptibility

The inhibition zone diameters of 10 antibiotics for ST12 and GT12 were explored. Antibiotic susceptibility testing showed that both ST12 and GT12 were susceptible to the 10 antibiotics (SXT, CIP, LEV, TZP, SCF, IPM, ATM, FEP, AK and MEM) according to criteria in the CLSI M100-S24 document[26] (Figure 2).

Biofilm Formation Ability

OD at 570 nm was taken for each strain to determine the quantity of biofilm formed. The OD_{570} of ST12 was lower than that of GT12 ($p = 0.0174$), suggesting that ST12 experienced a decreased biofilm formation ability, in contrast to GT12 (Figure 3).

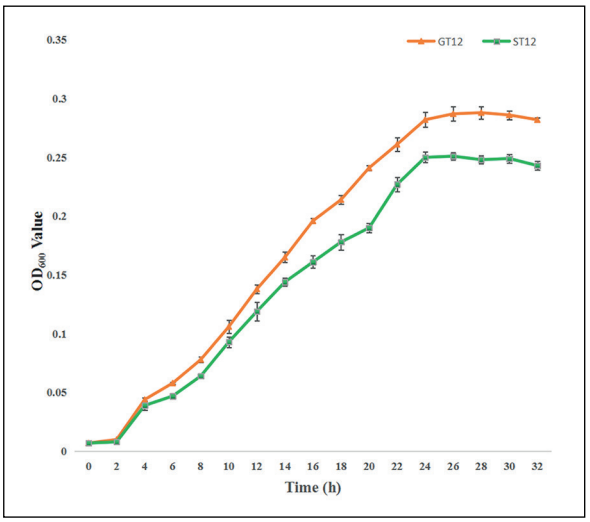

Figure 1. Growth curves of the ST12 and GT12. The growth curves of ST12 (green) and GT12 (red) were constructed by measuring OD_{600} values every 2 h for a period of 32 h; these values represent the bacterial concentration. The data showed that ST12 exhibited a reduced growth rate, in contrast to GT12.

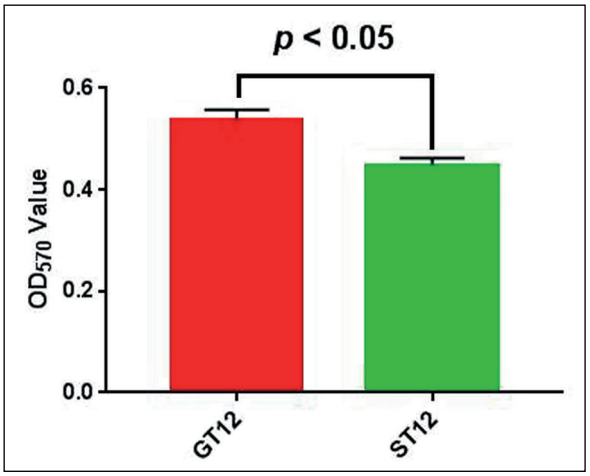

Figure 3. Biofilm formation ability of ST12 and GT12. Biofilm formation ability was analyzed by crystal violet staining. OD_{570} readings were taken to measure the thickness of the biofilm for each strain. The results showed that ST12 exhibited a decreased biofilm formation ability in comparison to GT12.

Whole-Genome Sequencing and Annotation

H3 was used as a reference strain for ST12 and GT12. The accession number of H3 was CP030754-CP030758. The draft genome of H3 was estimated to be approximately 3260417 bp. There were 3190 identified genes with a total length of 2760036 bp, which composed 84.65% of the genome. In addition, 17512 bp of the tandem repeat sequences and 2710 bp of the transposon sequences were identified, which compose 0.54% and 0.08% of the genome, respectively. Moreover, 87 tRNA fragments with a total length of 6792 bp and 2 snRNA genes with a total length of 166 bp were identified.

All the genes were annotated against 5 popular functional databases: 67.99% of the genes to the GO database, 69.84% of the genes into the COG database, 56.68% of the genes to KEGG, 94.86% of the genes to the NR database and 44.20% genes to SwissProt. The genome map of the reference strain H3 is shown in Figure 4.

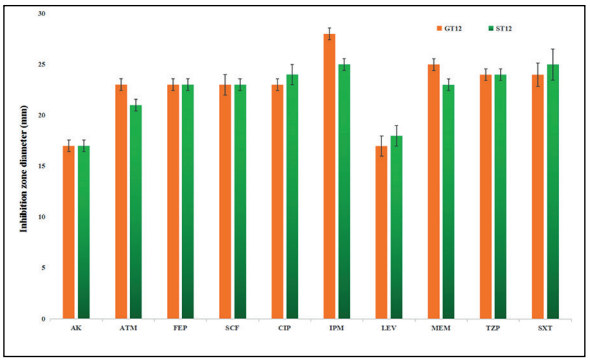

Figure 2. Antibiotic susceptibility test. Antibiotic susceptibility was determined by the disk diffusion test, and the inhibition zone diameter was measured for each antibiotic. The results indicated that both ST12 (green) and GT12 (red) were susceptible to 10 antibiotics.

Comparative Genomic Analysis

The accession numbers of DNA sequencing data for ST12 and GT12 were SRR7415023 and SRR7415022, respectively. H3 was used as a reference strain, and changes in ST12 and GT12, including SNPs and InDels, were identified (Figure 5).

SNPs

Two SNPs of GT12 were detected and were located in the functional genes H3GM000672 and H3GM002115**.** One SNP mutation in H3GM000672 was a nonsynonymous substitution of the gene *pilJ,* which plays an important role in biofilm formation. The other SNP mutation in H3GM002115 was annotated in an *iclR* family gene related to a DNA-binding transcriptional regulator in the COG database. However, no SNP was found in ST12.

Figure 4. Genome map of reference strain H3. From the outer to the inner circles, the 1st and 2nd circles represent coding gene sequences of the H3 strain; the 3rd and 4th circles represent COG annotations; the 5th and 6th circles represent ncRNA genes; the 7th circle represents GC content; and the 8th circle represents GC skew (G-C)/(G + C).

InDels

In total, 13 InDels in gene coding regions were identified for both ST12 and GT12 (Table I). Among these InDels, 1 insertion located in H3GM002670 was identified only in GT12, and the sequence contained a hypothetical gene with unknown functions.

RNA-Seq Mapping and Comparative Transcriptomic Analysis

The accession numbers of RNA sequencing data for ST12 and GT12 were SRR7410978 and SRR7410979, respectively. Compared with GT12, 1857 DEGs were identified in ST12, including

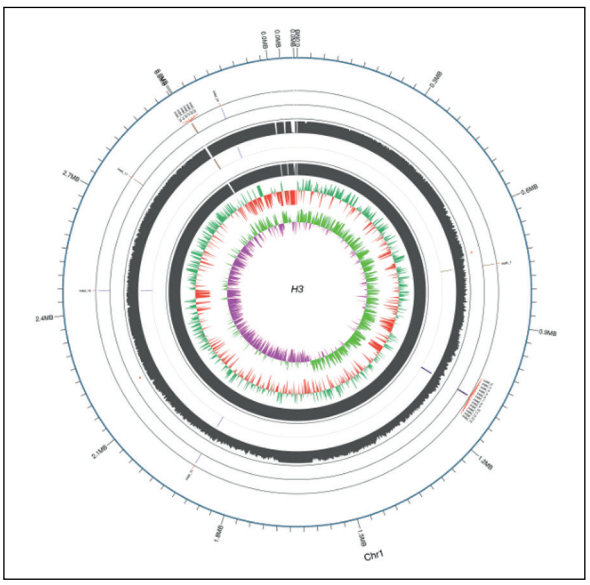

Figure 5. Comparative genomic analysis. From the outer to the inner circles, the 1st circle represents the InDels between H3 and GT12 (black: insertion, blue: deletion); the red spots represent the SNP mutation positions of GT12, which were annotated to the genes pilJ and iclR; the 2nd circle represents the coverage depth of the reads for GT12; the 3rd circle represents the Indels between H3 and ST12 (black: insertion, blue: deletion); the 4th circle represents the coverage depth of the reads for ST12; the 5th circle represents the GC content of H3; and the 6th circle represents the GC skew of H3.

Table I. Comparative analysis of InDels identified in ST12 and GT12.

Type	GT12			ST12			
	Position	Start	End	Position	Start	End	Gene ID
Insert 1	743794	743653	743796	743794	743653	743796	H3GM000710
Insert 2	1099365	1099035	1099373	1099365	1099035	1099373	H3GM001059 azaleucine resistance protein AzlC
Insert 3	1100924	1100917	1101006	1100924	1100917	1101006	H3GM001063
Insert 4	1101487	1101433	1101615	1101487	1101433	1101615	H3GM001064
Insert 5	1101609	1101433	1101615	1101609	1101433	1101615	H3GM001064
Insert 6	2767977	2767669	2768001				H3GM002670 hypothetical protein
Insert 7	140	27	197	140	27	197	H3GM002870
Insert 8	196	27	197	196	27	197	H3GM002870
Insert 9	2486	2462	2773	2486	2462	2773	H3GM002872 transposase
Delete 1	1099469	1099431	1099787	1099469	1099431	1099787	H3GM001060 hypothetical protein
Delete 2	2457719	2457554	2457769	2457719	2457554	2457769	H3GM002371
Delete 3	88332	87965	88339	88332	87965	88339	H3GM002960 imidazole glycerol phosphate synthase subunit hisF
Delete 4	88332	88311	88724	88332	88311	88724	H3GM002961 imidazole glycerol phosphate synthase subunit hisF

590 upregulated genes and 1267 downregulated genes.

A cluster analysis of the DEGs between ST12 and GT12 is shown in Figure 6. The ratio of downregulated genes to upregulated genes was approximately 2.1, suggesting that gene expression was inhibited in ST12.

GO Analysis

In total, 30 categories including 1162 DEGs (identical DEGs may fall into different categories) were identified between ST12 and GT12 according to the GO function classification. Compared with GT12, ST12 was characterized by the regulation of a number of genes related to intracellular organelle ($p = 0.0460$), cation binding ($p = 0.0285$) and metal iron binding ($p = 0.0357$) (Figure 7). Notably, DEGs involved in metal iron binding included many upregulated genes, and these genes might be related to biofilm formation (Figure 8).

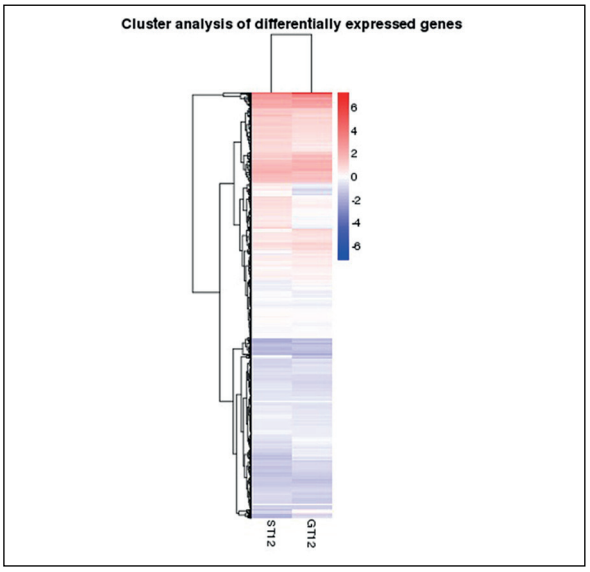

Figure 6. Hierarchical clustering analysis of DEGs. The heatmap was generated from a hierarchical cluster analysis of genes. Red bars represent the upregulated genes and blue bars represent the downregulated genes.

COG Analysis

For COG analysis, 460 DEGs (identical DEGs may fall into different categories) were categorized into 21 COG functional classes. Most changes were annotated in two COG categories, namely, the amino acid transport and metabolism category and the translation, ribosomal structure and biogenesis category (Figure 9). The former category included 65 DEGs, and the latter category included 69 DEGs. Notably, 10 downregulated genes were identified in the cell wall/membrane/envelope biogenesis category, and some of these genes encoded glycosyltransferases that participate in the synthesis of the cell membrane. In addition, 12 DEGs involved in the energy production and conversion were downregulated, including genes encoding NADH reductase, acetate kinase and lactate dehydrogenase.

Antibiotic Resistance Analysis

A total of 11 DEGs associated with antibiotic resistance were identified in ST12 compared with

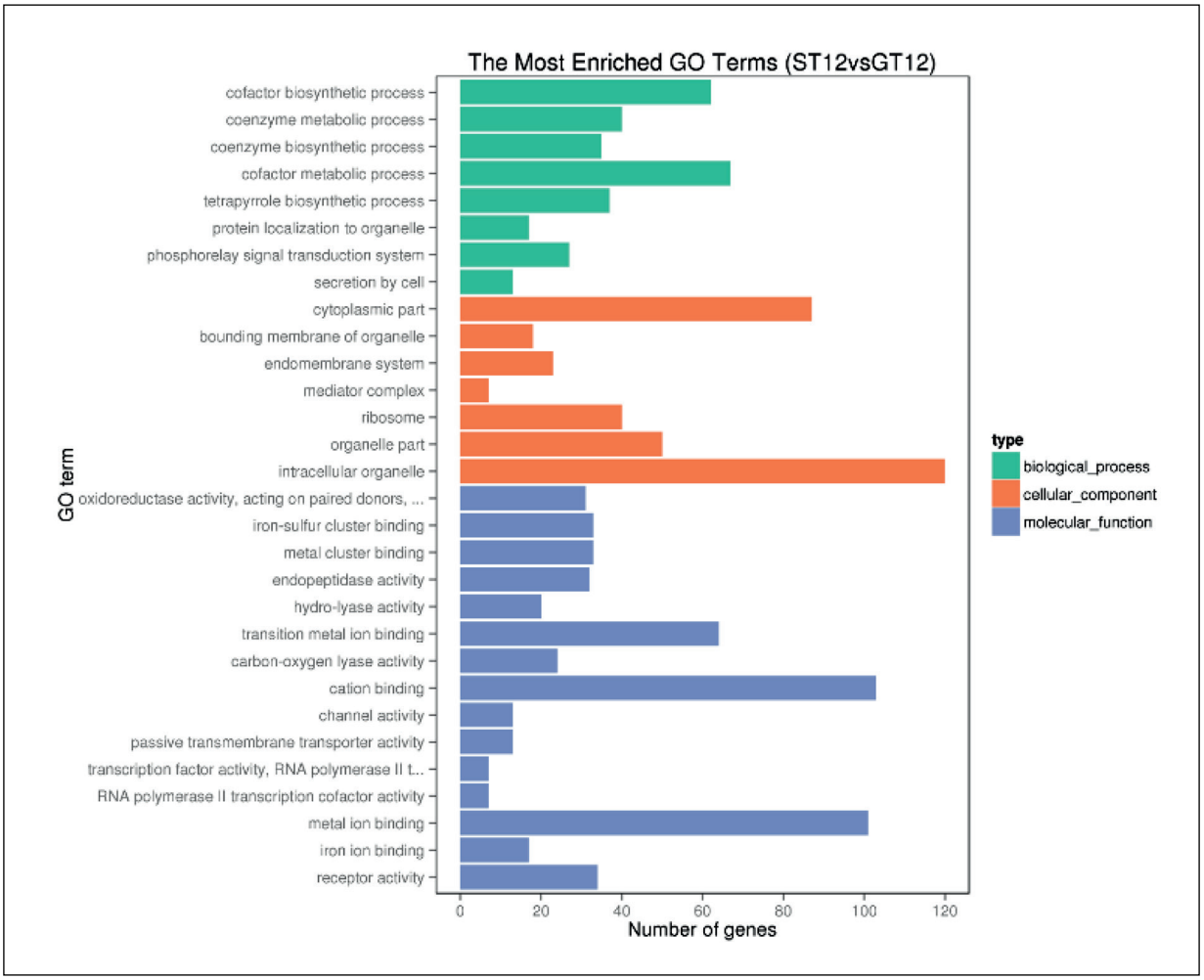

Figure 7. Distribution of DEGs in GO functional classification. The X-axis represents the number of DEGs according to GO functional classification. The Y-axis represents the item of GO functional classification.

GT12 (Table II). Of these genes, 3 DEGs, namely *acrA*, *adeC* and *smeE,* were upregulated, and the other 8 DEGs were downregulated. The *acrA* and *smeE* genes regulated a multidrug resistance efflux pump, which contributes to resistance against fluoroquinolone antibiotics. The *adeC* gene is related to aminoglycoside resistance.

Virulence Analysis

Using the VFDB-based annotation system, 39 genes performing transcriptomic changes were identified in ST12 in contrast with GT12 (Table II). Among these DEGs, 8 genes were upregulated, and 31 genes were downregulated. Strikingly, some downregulated genes, including *pilB, pilD, pilG, pilH, pilJ, pilM, pilO, pilQ, pilT, pilU,* and *algR,* were related to type IV pili, which play important roles in the process of biofilm formation.

Discussion

To the best of our knowledge, this is the first study on *A. schindleri* after a long-duration spaceflight. It thus represents a breakthrough regarding phenotypic changes and relative mechanisms of *A. schindleri* after long flights. The key finding of this study is that *A. schindleri* exhibits a decreased growth rate and biofilm formation ability after a long spaceflight. Furthermore, comparative genomic and transcriptomic analyses indicate that these phenotypic alternations are associated with some gene mutations and gene expression changes.

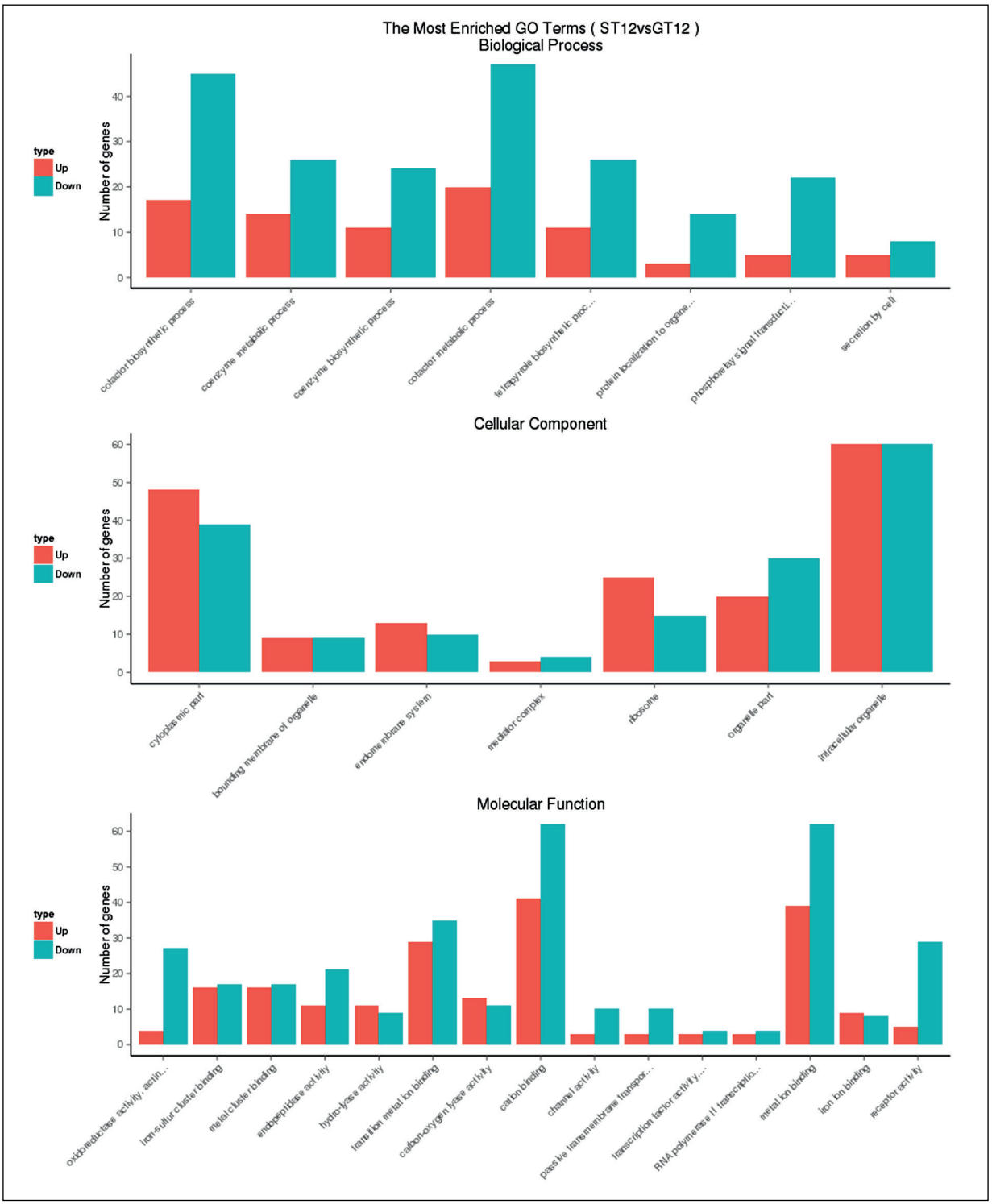

Figure 8. Distribution of the upregulated and downregulated DEGs in GO functional classification. Blue bars represent the downregulated DEGs, and red bars represent the upregulated DEGs. The X-axis represents the item of GO functional classification. The Y-axis represents the number of DEGs according to GO functional classification.

The adaptation of bacteria to the space environment may be determined by the growth rate of the strains. It has been reported that bacteria exposed to modeled microgravity and the space environment tend to exhibit different growth rates, which are based on growth phase, motility

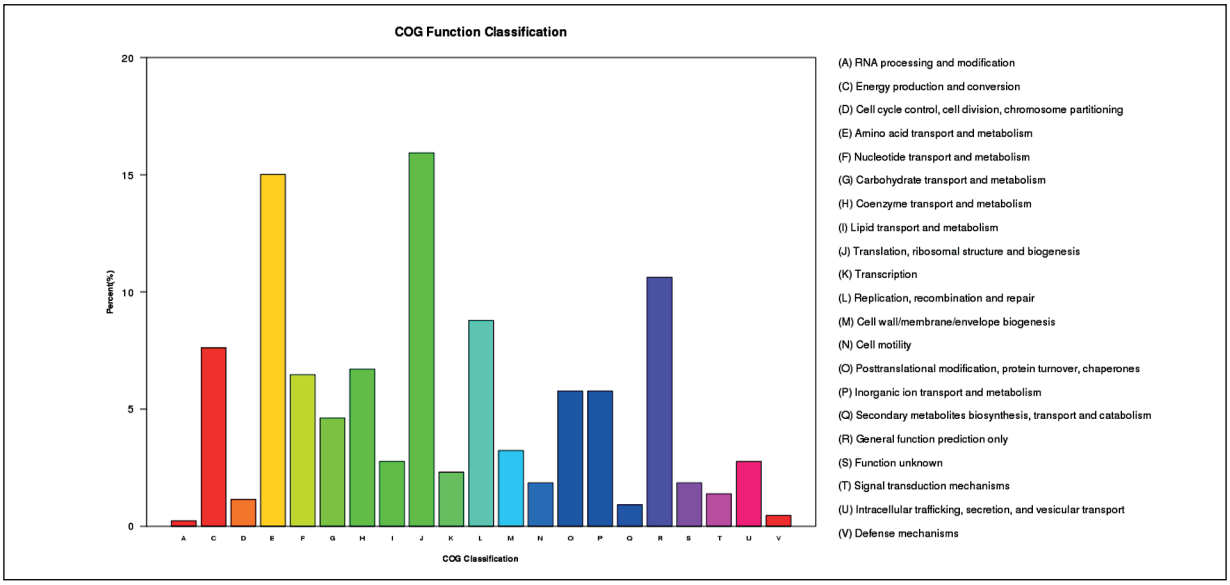

Figure 9. Distribution of the DEGs in COG functional classification. The X-axis represents the COG functional category. The Y-axis represents the percentage of genes in each COG category.

mode, culture method and culture medium concentration[6,27,28]. In this analysis, the growth curve of ST12 was lower than that of GT12, suggesting that *A. schindleri* experienced a decreased growth rate after a longer spaceflight. Previous studies[29,30] indicated that spaceflight altered the microenvironment surrounding microorganisms and then affected their transport and utilization of nutrients, ultimately leading to changes in the growth rate of the microorganisms. Differences in mass diffusion of the cellular microenvironment could alter the metabolic reactions of bacteria[31]. In this study, the diminished growth rate of ST12 might have been associated with the DEGs involved in the amino acid transport and metabolism category according to the COG function classification. The same change in growth rate was also found in a recent study of *Staphylococcus epidermidis* during spaceflight, and the difference in nutrient diffusion between the flight group and the ground control group might play an important role in the process[32]. Moreover, based on the COG functional classification, 12 downregulated genes in the energy production and conversion category were identified in ST12, and these genes might also play a critical part in the decreased growth rate of ST12. In addition, the cell membrane might provide the best protection of cell integrity under stress conditions[20]. In this study, 10 genes associated with cell wall/membrane/envelope biogenesis were downregulated in ST12 on the basis of the COG functional classification. As such, it was speculated that this response, together with the downregulated genes

Table II. DEGs associated with antibiotic resistance.

Gene ID	Gene	Expression	*p*-value	Gene function
H3GM000714	*adeC*	Up	2.83e-06	Multidrug resistance efflux pump
H3GM000715	*smeE*	Up	4.90e-21	Multidrug resistance efflux pump
H3GM000716	*acrA*	Up	1.64e-14	Multidrug resistance efflux pump
H3GM000180	*aph*	Down	4.88e-27	Aminoglycoside O-phosphotransferase
H3GM000321	*mdfA*	Down	5.21e-10	-
H3GM000787	*mexB*	Down	0.0001615	Multidrug resistance efflux pump
H3GM000964	*bacA*	Down	6.23e-05	Undecaprenyl pyrophosphate phosphatase
H3GM001418	*emrE*	Down	0.0033788	Multidrug resistance efflux pump
H3GM001440	*rosA*	Down	2.09e-07	Major facilitator superfamily transporter
H3GM002324	*macB*	Down	8.22e-17	Macrolide-specific efflux system
H3GM002422	*rosB*	Down	3.70e-06	Potassium antiporter

Table III. DEGs in the VFDB-based annotation system.

Gene ID	Gene	Expression	*p*-value	Gene function
H3GM000071	*tviB*	Down	2.45e-10	Increase resistance to host peroxide and complement activation
H3GM000082	*bplL*	Down	2.68e-06	Prevent clearance of the organism and confer protection to the bacterium
H3GM000088	*galE*	Down	1.14e-06	Colonize Peyer's patches and affect the virulence factors expression
H3GM000089	*manB*	Down	1.17e-06	Colonize Peyer's patches and affect the virulence factors expression
H3GM000200	*pilR*	Down	0.00085	Attach to host cells and cause a twitching motility; Biofilm formation
H3GM000232	*pilD*	Down	0.00555	Contribute to complement-independent binding
H3GM000234	*pilB*	Down	2.16e-10	Attach to host cells and cause twitching motility; Biofilm formation
H3GM000268	*pilM*	Down	9.77e-13	Attach to host cells and cause twitching motility; Biofilm formation
H3GM000270	*pilO*	Down	4.25e-06	Attach to host cells and cause twitching motility; Biofilm formation
H3GM000272	*pilQ*	Down	3.18e-40	Attach to host cells and cause twitching motility; Biofilm formation
H3GM000669	*pilG*	Down	4.59e-05	Attach to host cells and cause twitching motility; Biofilm formation
H3GM000670	*pilH*	Down	0.00828	Attach to host cells and cause twitching motility; Biofilm formation
H3GM000672	*pilJ*	Down	3.72e-19	Attach to host cells and cause twitching motility; Biofilm formation
H3GM001004	*xcpR*	Down	0.00214	Secrete toxins and enzymes into the extracellular fluid
H3GM001030	*csrA*	Down	1.06e-17	Posttranscriptional repression of the transmission regulon
H3GM001112	ahpC	Down	1.95e-11	Protecting mycobacteria from the oxidative responses of macrophages
H3GM001354	*pilU*	Down	0.00161	Attach to host cells and cause twitching motility; Biofilm formation
H3GM001355	*pilU*	Down	1.30e-07	Attach to host cells and cause twitching motility; Biofilm formation
H3GM001360	*ybtP*	Down	2.07e-07	Remove iron from a number of mammalian proteins
H3GM001377	*ureG*	Down	1.11e-08	Contribute to acid resistance, chemotactic behavior, and nitrogen metabolism
H3GM001379	*ureA*	Down	0.00037	Contribute to acid resistance, chemotactic behavior, and nitrogen metabolism
H3GM001381	*ureB*	Down	1.30e-20	Contribute to acid resistance, chemotactic behavior, and nitrogen metabolism
H3GM001507	*PA0084*	Down	1.98e-06	Play a role in chronic P. aeruginosa infections
H3GM001985	*clpV*	Down	1.35e-11	Play a role in chronic P. aeruginosa infections
H3GM002132	*pilT*	Down	2.20e-06	Attach to host cells and cause twitching motility; Biofilm formation
H3GM002133	*pilU*	Down	0.00198	Attach to host cells and cause twitching motility; Biofilm formation
H3GM002239	*xcpR*	Down	0.00369	Secrete toxins and enzymes into the extracellular fluid
H3GM002284	*hasB*	Down	0.01759	Promote tissue penetration by GAS through a paracellular route
H3GM002293	*panC*	Down	0.01871	Pantothenate biosynthesis
H3GM002528	*xcpT*	Down	2.70e-07	Secrete toxins and enzymes into the extracellular fluid
H3GM002529	*xcpS*	Down	7.02e-06	Secrete toxins and enzymes into the extracellular fluid
H3GM002600	*algR*	Down	0.00012	Allow the bacteria to form a biofilm
H3GM002949	*mprA*	Down	0.01128	Establishment and maintenance of persistent infection
H3GM000323	*sodC*	Up	5.88e-07	Contribute to survival during the systemic phase of infection
H3GM000492	*relA*	Up	5.02e-13	Convert the alveolar macrophages from a replicated to a virulent state
H3GM000745	*panD*	Up	0.00570	Lipid biosynthesis and metabolism
H3GM000760	*kdtB*	Up	2.27e-05	Prolong H. pylori infection for longer and mediate a lectin-like interaction
H3GM001555	*clpE*	Up	1.03e-60	Act synergistically with ClpC in cell division
H3GM001786	*clpC*	Up	2.41e-15	Promote early escape form the phagosome of macrophages
H3GM002134	*fur*	Up	0.00017	Repress the expression of iron-regulated genes
H3GM002557	*mprB*	Up	0.00609	Establishment and maintenance of persistent infection

in transmembrane transport and energy production and conversion, might induce the diminished growth rate of *A. schindleri* after a long-duration spaceflight.

In general, the antibiotic susceptibility of bacteria is attributed to their ability to acquire and express a wide range of antibiotic susceptibility-associated genes. It has been reported that the space environment affects the antibiotic susceptibility of microbes during spaceflight[29]. Some evidence[33] indicates that gene mutation is a common mechanism by which microbes become resistant to antibiotics. It is almost certain that the gene mutations of microbes would affect the absorption, distribution, metabolism, and elimination of antibiotics during space missions[11]. Exposure to the space environment causes unique stresses on microbes, motivating the microbial potential for gene mutations, which in turn may ultimately causing decreased antibiotic effectiveness. For

example, a recent analysis indicated that *S. epidermidis* exhibited stronger resistance to rifampicin in the space environment compared with that at ground control, and the higher mutation rates of the *rpoB* gene during spaceflight led to rifampicin resistance[32]. However, some studies indicated that the bacteria did not develop a higher level of antibiotic resistance due to exposure to the space environment[34]. In this study, the antibiotic susceptibility test showed that both ST12 and GT12 were susceptible to 10 antibiotics, namely SXT, CIP, LEV, TZP, SCF, IPM, ATM, FEP, AK, and MEM, suggesting that *A. schindleri* remained susceptible to these antibiotics after a long-duration spaceflight. Transcriptomic analysis showed that drug resistance-associated genes, including *acrA*, *adeC*, and *smeE,* were upregulated in ST12 according to the ARDB database. These genes encode an active efflux pump that facilitates a high resistance to fluoroquinolones and aminoglycosides[35-37]. Although the *acrA, adeC,* and *smeE* genes were overexpressed in ST12, no gene mutation associated with drug resistance was detected in ST12 from the comparative genomic analysis. This result explained why *A. schindleri* did not lose its drug-susceptible phenotype with regard to these antibiotics after a long-duration spaceflight.

A biofilm is a special aggregate of microbial cells that attaches to the surface of organisms and materials and is surrounded by an extracellular matrix that consists of polysaccharides, DNA and proteins[38]. Biofilms appear at the solid-liquid and air-liquid interfaces and confer protection from the environmental hazards[39]. On the one hand, biofilms attaching to the surface of medical devices and body tissues play an important role in drug resistance to antibacterial treatment[40]. On the other hand, biofilms could dramatically aggravate the corrosion of materials and equipment by bacteria[41,42]. Previous studies have demonstrated that bacteria tend to exhibit diverse biofilm phenotypes under modeled microgravity and in the space environment. For example, a modeled microgravity strain of *Klebsiella pneumonia* showed an enhanced biofilm formation ability, while another spaceflight strain of *Acinetobacter baumannii* showed a decreased biofilm formation ability compared with the ground control[43,44]. Considering that astronauts will stay on the space station for a long time, it is necessary to analyze bacterial biofilm-forming ability after a long-duration spaceflight. In this study, ST12 produced less biofilms than GT12, indicating that *A. schindleri* exhibited a weaker ability to form biofilms after a long-duration spaceflight. One factor contributing to this phenomenon might be the downregulated genes including *pilB, pilD, pilG, pilH, pilJ, pilM, pilO, pilQ, pilT, pilU,* and *algR* in ST12. The *pil* genes encode pilin-like proteins associated with type IV pili, which are important for biofilm formation in multiple species[45-47]. The *algR* gene encodes the alginate biosynthesis protein AlgR which is related to the virulence and biofilm formation of bacteria[48]. It was hypothesized that the downregulated expression of *pil* and *algR* could decrease the biofilm formation ability of ST12. Also, previous investigations have reported that the PilJ protein demonstrated its incorporation into type IV pili and played an important role in swarming motility, cellular adhesion and biofilm formation[49]. Therefore, the mutation of the *pilJ* gene in GT12 might also result in an altered level of biofilm production compared to that of ST12. Moreover, iron availability affects swarming motility and biofilm formation in various microorganisms, and the addition of ferric iron leads to increased biofilm formation. Lin et al[50] showed that chelate ferric iron silenced RssAB signaling and triggered swarming initiation and biofilm reduction. Therefore, it was speculated that the decreased biofilm formation of ST12 might be attributed to the upregulated expression of genes associated with metal iron binding according to the GO analysis.

Conclusions

This study presents the data only available to analyze the various effects of a long-duration spaceflight on *A. schindleri.* The results indicate that the DEGs of the strain during a long-duration spaceflight are one of the important factors resulted in the decreased growth rate and biofilm formation ability of *A. schindleri*. These findings may improve our ability to understand how microbes will adapt to a long-duration spaceflight.

China launched the Tiangong-2 space lab in 2016 and will eventually build a space station by the early 2020s. Considering that one of the new challenges facing astronauts is to reach increasingly long-duration spaceflight targets, it can be reasoned that studying the influences of long-duration spaceflight exposure on microbial behavior, such as growth rate, biofilm formation, antibiotic susceptibility and virulence, is necessary for predicting the possible pathogenesis mechanisms,

providing the treatment of infectious diseases and maintaining the safety of the space station. In addition, more attention should be paid to the host-microbe interactions during long-duration spaceflight. In a word, future research may be conducted to establish a space microbiological safety assessment system to protect the health of crew members and ensure the safe operation of space station.

Conflict of Interest

The Authors declare that they have no conflict of interests.

Acknowledgements

We gratefully thank the China Astronaut Research and Training Center for payload hardware preparation.

Funding

This work was funded by the National Basic Research Program of China (2014CB744400), the National Significant Science Foundation (No. 2015ZX09J15102-003), and the Key Program of Logistics Research (BWS17J030).

References

1) Singh NK, Wood JM, Karouia F, Venkateswaran K. Succession and persistence of microbial communities and antimicrobial resistance genes associated with International Space Station environmental surfaces. Microbiome 2018; 6: 204.
2) Checinska SA, Urbaniak C, Mohan G, Stepanov VG, Tran Q, Wood JM, Minich J, McDonald D, Mayer T, Knight R, Karouia F, Fox GE, Venkateswaran K. Characterization of the total and viable bacterial and fungal communities associated with the International Space Station surfaces. Microbiome 2019; 7: 50.
3) Urbaniak C, Sielaff AC, Frey KG, Allen JE, Singh N, Jaing C, Wheeler K, Venkateswaran K. Detection of antimicrobial resistance genes associated with the International Space Station environmental surfaces. Sci Rep 2018; 8: 814.
4) Gao H, Liu Z, Zhang L. Secondary metabolism in simulated microgravity and space flight. Protein Cell 2011; 2: 858-861.
5) Kim W, Tengra FK, Shong J, Marchand N, Chan HK, Young Z, Pangule RC, Parra M, Dordick JS, Plawsky JL, Collins CH. Effect of spaceflight on Pseudomonas aeruginosa final cell density is modulated by nutrient and oxygen availability. BMC Microbiol 2013; 13: 241.
6) Byloos B, Coninx I, Van Hoey O, Cockell C, Nicholson N, Ilyin V, Van Houdt R, Boon N, Leys N. The Impact of Space Flight on Survival and Interaction of Cupriavidus metallidurans CH34 with Basalt, a Volcanic Moon Analog Rock. Front Microbiol 2017; 8: 671.
7) Senatore G, Mastroleo F, Leys N, Mauriello G. Effect of microgravity & space radiation on microbes. Future Microbiol 2018; 13: 831-847.
8) Foster JS, Wheeler RM, Pamphile R. Host-microbe interactions in microgravity: assessment and implications. Life (Basel) 2014; 4: 250-266.
9) Liu C. The theory and application of space microbiology: China's experiences in space experiments and beyond. Environ Microbiol 2017; 19: 426-433.
10) Yamaguchi N, Roberts M, Castro S, Oubre C, Makimura K, Leys N, Grohmann E, Sugita T, Ichijo T, Nasu M. Microbial monitoring of crewed habitats in space-current status and future perspectives. Microbes Environ 2014; 29: 250-260.
11) Taylor PW. Impact of space flight on bacterial virulence and antibiotic susceptibility. Infect Drug Resist 2015; 8: 249-262.
12) Kee C, Junqueira A, Uchida A, Purbojati RW, Houghton J, Chenard C, Wong A, Clare ME, Kushwaha KK, Panicker D, Putra A, Gaultier NE, Premkrishnan B, Heinle CE, Vettath VK, Drautz-Moses DI, Schuster SC. Complete genome sequence of Acinetobacter schindleri SGAir0122 isolated from Singapore air. Genome Announc 2018; 6: e00567-18.
13) Montana S, Palombarani S, Carulla M, Kunst A, Rodriguez CH, Nastro M, Vay C, Ramirez MS, Almuzara M. First case of bacteraemia due to Acinetobacter schindleri harbouring blaNDM-1 in an immunocompromised patient. New Microbes New Infect 2018; 21: 28-30.
14) Crucian BE, Chouker A, Simpson RJ, Mehta S, Marshall G, Smith SM, Zwart SR, Heer M, Ponomarev S, Whitmire A, Frippiat JP, Douglas GL, Lorenzi H, Buchheim JI, Makedonas G, Ginsburg GS, Ott CM, Pierson DL, Krieger SS, Baecker N, Sams C. Immune system dysregulation during spaceflight: potential countermeasures for deep space exploration missions. Front Immunol 2018; 9: 1437.
15) Dortet L, Legrand P, Soussy CJ, Cattoir V. Bacterial identification, clinical significance, and antimicrobial susceptibilities of Acinetobacter ursingii and Acinetobacter schindleri, two frequently misidentified opportunistic pathogens. J Clin Microbiol 2006; 44: 4471-4478.
16) Crucian BE, Stowe RP, Pierson DL, Sams CF. Immune system dysregulation following short- vs long-duration spaceflight. Aviat Space Environ Med 2008; 79: 835-843.
17) Urbaniak C, Reid G. The potential influence of the microbiota and probiotics on women during long spaceflights. Womens Health (Lond) 2016; 12: 193-198.
18) Douglas GL, Voorhies AA. Evidence based selection of probiotic strains to promote astronaut health or alleviate symptoms of illness on long du-

ration spaceflight missions. Benef Microbes 2017; 8: 727-737.

19) Yin H, Xie SY, Zhang GM, Xie SM. [Effect of space flight on yield of Monascus purpureus]. Space Med Med Eng (Beijing) 2003; 16: 374-376.
20) Turton JF, Hyde R, Martin K, Shah J. Genes encoding OXA-134-like enzymes are found in Acinetobacter lwoffii and A. schindleri and can be used for identification. J Clin Microbiol 2012; 50: 1019-1022.
21) Guo Y, Li Y, Su L, Chang D, Liu W, Wang T, Yuan Y, Fang X, Wang J, Li T, Fang C, Dai W, Liu C. Comparative genomic analysis of Klebsiella pneumonia (LCT-KP214) and a mutant strain (LCT-KP289) obtained after spaceflight. BMC Genomics 2014; 15: 589.
22) Berlin K, Koren S, Chin CS, Drake JP, Landolin JM, Phillippy AM. Assembling large genomes with single-molecule sequencing and locality-sensitive hashing. Nat Biotechnol 2015; 33: 623-630.
23) Koren S, Phillippy AM. One chromosome, one contig: complete microbial genomes from long-read sequencing and assembly. Curr Opin Microbiol 2015; 23: 110-120.
24) Krzywinski M, Schein J, Birol I, Connors J, Gascoyne R, Horsman D, Jones SJ, Marra MA. Circos: an information aesthetic for comparative genomics. Genome Res 2009; 19: 1639-1645.
25) Langmead B, Salzberg SL. Fast gapped-read alignment with Bowtie 2. Nat Methods 2012; 9: 357-359.
26) Danilenko U, Vesper HW, Myers GL, Clapshaw PA, Camara JE, Miller WG. An updated protocol based on CLSI document C37 for preparation of off-the-clot serum from individual units for use alone or to prepare commutable pooled serum reference materials. Clin Chem Lab Med 2020; 58: 368-374.
27) Baker PW, Leff L. The effect of simulated microgravity on bacteria from the Mir space station. Microgravity Sci Technol 2004; 15: 35-41.
28) Vukanti R, Model MA, Leff LG. Effect of modeled reduced gravity conditions on bacterial morphology and physiology. BMC Microbiol 2012; 12: 4.
29) Klaus DM, Howard HN. Antibiotic efficacy and microbial virulence during space flight. Trends Biotechnol 2006; 24: 131-136.
30) Brown RB, Klaus D, Todd P. Effects of space flight, clinorotation, and centrifugation on the substrate utilization efficiency of E. coli. Microgravity Sci Technol 2002; 13: 24-29.
31) Nickerson CA, Ott CM, Wilson JW, Ramamurthy R, Pierson DL. Microbial responses to microgravity and other low-shear environments. Microbiol Mol Biol Rev 2004; 68: 345-361.
32) Fajardo-Cavazos P, Nicholson WL. Cultivation of Staphylococcus epidermidis in the human spaceflight environment leads to alterations in the frequency and spectrum of spontaneous rifampicin-resistance mutations in the rpoB gene. Front Microbiol 2016; 7: 999.
33) Nicholson WL, Park R. Anaerobic growth of Bacillus subtilis alters the spectrum of spontaneous mutations in the rpoB gene leading to rifampicin resistance. FEMS Microbiol Lett 2015; 362: v213.
34) Morrison MD, Fajardo-Cavazos P, Nicholson WL. Cultivation in space flight produces minimal alterations in the susceptibility of Bacillus subtilis cells to 72 different antibiotics and growth-inhibiting compounds. Appl Environ Microbiol 2017; 83: e01584-17.
35) Zhou X, Jia F, Liu X, Wang Y. Total alkaloids of Sophorea alopecuroides-induced down-regulation of AcrAB-TolC efflux pump reverses susceptibility to ciprofloxacin in clinical multidrug resistant Escherichia coli isolates. Phytother Res 2012; 26: 1637-1643.
36) Jia W, Wang J, Xu H, Li G. Resistance of Stenotrophomonas maltophilia to fluoroquinolones: prevalence in a university hospital and possible mechanisms. Int J Environ Res Public Health 2015; 12: 5177-5195.
37) Modarresi F, Azizi O, Shakibaie MR, Motamedifar M, Valibeigi B, Mansouri S. Effect of iron on expression of efflux pump (adeABC) and quorum sensing (luxI, luxR) genes in clinical isolates of Acinetobacter baumannii. APMIS 2015; 123: 959-968.
38) Richmond GE, Evans LP, Anderson MJ, Wand ME, Bonney LC, Ivens A, Chua KL, Webber MA, Sutton JM, Peterson ML, Piddock LJ. The Acinetobacter baumannii two-component system AdeRS regulates genes required for multidrug efflux, biofilm formation, and virulence in a strain-specific manner. Mbio 2016; 7: e416-e430.
39) Marti S, Rodriguez-Bano J, Catel-Ferreira M, Jouenne T, Vila J, Seifert H, De E. Biofilm formation at the solid-liquid and air-liquid interfaces by Acinetobacter species. BMC Res Notes 2011; 4: 5.
40) Anbazhagan D, Mansor M, Yan GO, Md YM, Hassan H, Sekaran SD. Detection of quorum sensing signal molecules and identification of an autoinducer synthase gene among biofilm forming clinical isolates of Acinetobacter spp. PLoS One 2012; 7: e36696.
41) Gu JD, Roman M, Esselman T, Mitchell R. The role of microbial biofilms in deterioration of space station candidate materials. Int Biodeterior Biodegradation 1998; 41: 25-33.
42) Zea L, Nisar Z, Rubin P, Cortesao M, Luo J, McBride SA, Moeller R, Klaus D, Muller D, Varanasi KK, Muecklich F, Stodieck L. Design of a spaceflight biofilm experiment. Acta Astronaut 2018; 148: 294-300.
43) Wang H, Yan Y, Rong D, Wang J, Wang H, Liu Z, Wang J, Yang R, Han Y. Increased biofilm formation ability in Klebsiella pneumoniae after short-term exposure to a simulated microgravity environment. Microbiologyopen 2016; 5: 793-801.
44) Zhao X, Yu Y, Zhang X, Huang B, Bai P, Xu C, Li D, Zhang B, Liu C. Decreased biofilm formation ability of Acinetobacter baumannii after spaceflight on China's Shenzhou 11 spacecraft. Microbiologyopen 2019; 8: e763.
45) Whitchurch CB, Leech AJ, Young MD, Kennedy D, Sargent JL, Bertrand JJ, Semmler AB, Mellick

AS, Martin PR, Alm RA, Hobbs M, Beatson SA, Huang B, Nguyen L, Commolli JC, Engel JN, Darzins A, Mattick JS. Characterization of a complex chemosensory signal transduction system which controls twitching motility in Pseudomonas aeruginosa. Mol Microbiol 2004; 52: 873-893.

46) Piepenbrink KH, Maldarelli GA, de la Pena CF, Mulvey GL, Snyder GA, De Masi L, von Rosenvinge EC, Gunther S, Armstrong GD, Donnenberg MS, Sundberg EJ. Structure of Clostridium difficile PilJ exhibits unprecedented divergence from known type IV pilins. J Biol Chem 2014; 289: 4334-4345.

47) Maldarelli GA, Piepenbrink KH, Scott AJ, Freiberg JA, Song Y, Achermann Y, Ernst RK, Shirtliff ME, Sundberg EJ, Donnenberg MS, von Rosenvinge EC. Type IV pili promote early biofilm formation by Clostridium difficile. Pathog Dis 2016; 74: ftw061.

48) Redelman CV, Chakravarty S, Anderson GG. Antibiotic treatment of Pseudomonas aeruginosa biofilms stimulates expression of the magnesium transporter gene mgtE. Microbiology (Reading) 2014; 160: 165-178.

49) Kamath KS, Pascovici D, Penesyan A, Goel A, Venkatakrishnan V, Paulsen IT, Packer NH, Molloy MP. Pseudomonas aeruginosa cell membrane protein expression from phenotypically diverse cystic fibrosis isolates demonstrates host-specific adaptations. J Proteome Res 2016; 15: 2152-2163.

50) Lin CS, Tsai YH, Chang CJ, Tseng SF, Wu TR, Lu CC, Wu TS, Lu JJ, Horng JT, Martel J, Ojcius DM, Lai HC, Young JD. An iron detection system determines bacterial swarming initiation and biofilm formation. Sci Rep 2016; 6: 36747.